J|A|C|S
ARTICLES
Published on Web 02/16/2002

Ion Channel Formation from a Calix[4]arene Amide That Binds HCl

Vladimir Sidorov,*,† Frank W. Kotch,† Galya Abdrakhmanova,‡ Robert Mizani,§ James C. Fettinger,† and Jeffery T. Davis*,†

Contribution from the Department of Chemistry and Biochemistry, University of Maryland, College Park, Maryland 20742, Department of Pharmacology, 4000 Reservoir Road, Georgetown University, Washington, D.C., 20007, and Department of Biology, University of Maryland, College Park, Maryland 20742

Received October 11, 2001

Abstract: The ion transport activity of calix[4]arene tetrabutylamide *1,3-alt* **2** was studied in liposomes, planar lipid bilayers, and HEK-293 cells. These experiments, when considered together with ^{1}H NMR and X-ray crystallography data, indicate that calix[4]arene tetrabutylamide **2** (1) forms ion channels in bilayer membranes, (2) mediates ion transport across cell membranes at positive holding potential, (3) alters the pH inside liposomes experiencing a Cl^- gradient, and (4) shows a significant Cl^-/SO_4^{2-} transport selectivity. An analogue, calix[4]arene tetramethylamide **1**, self-assembles in the presence of HCl to generate solid-state structures with chloride-filled and water-filled channels. Structure−activity studies indicate that the hydrophobicity, amide substitution, and macrocyclic framework of the calixarene are essential for HCl binding and transport. Calix[4]arene tetrabutylamide **2** is a rare example of an anion-dependent, synthetic ion channel.

Introduction

Ion transport across membranes is one of the most important processes in living cells. Proteins that serve as ion channels or carriers provide this crucial activity.[1] The desire to understand these proteins, along with a need for new antibiotics,[2] has spurred development of ion channel models.[3] Although most synthetic channels have been designed for cation transport, there are some synthetic peptides that function as Cl^--selective ion channels.[4] These peptides have sequences corresponding to the transmembrane domains of anion channel proteins, such as the cystic fibrosis transmembrane conductance regulator (CFTR). There are fewer examples of nonpeptidic synthetic channels that interact with anions. Most notably, Regen has proposed that protonated amines in a spermine−steroid conjugate may facilitate Cl^- movement across a membrane bilayer.[5] Matile has indicated that rigid-rod polyols can mediate anion transport.[3d] Both these studies are encouraging for the development of new synthetic anion channels. While there has been significant progress in understanding the structure and function of natural and artificial cation channels, much less is known about anion channels.[6] Studying appropriate models may provide insight into the properties of natural anion channels.[7] Another rationale for developing synthetic anion channels is that these compounds may well control anion exchange processes in cells. For example, synthetic peptides can restore Cl^- transport in CFTR-deficient cells.[4e] In this paper, we describe a calixarene that forms a synthetic ion channel in a Cl^- dependent fashion.

Both single molecule and self-assembly approaches have been used to construct synthetic ion channels.[3] Self-assembly is an attractive approach for making pores within a membrane, as functional structures can arise from simple building blocks. Many synthetic cation channels have been made from compounds that presumably form the active structures by self-assembly. Nature certainly makes spectacular use of self-assembly to form ion channels, as illustrated by the crystal

† Department of Chemistry and Biochemistry, University of Maryland.
‡ Department of Pharmacology, Georgetown University.
§ Department of Biology, University of Maryland.

(1) (a) Hille, B. Ionic Channels of Excitable Membranes, 2nd ed.; Sinauer: Sunderland, MA, 1992. (b) Saier, M. H. *J. Membr. Biol.* **2000**, *175*, 165.
(2) (a) Fernandez-Lopez, S.; Kim, H. S.; Choi, E. C.; Delgado, M.; Granja, J. R.; Khasanov, A.; Kraehenbuehl, K.; Long, G.; Weinberger, D. A.; Wilcoxen, K. M.; Ghadiri, M. R. *Nature* **2001**, *412*, 452. (b) Porter, E. A.; Wang, X. F.; Lee, H. S.; Weisblum, B.; Gellman, S. H. *Nature* **2000**, *404*, 565. (c) Hamuro, Y.; Schneider, J. P.; DeGrado, W. F. *J. Am. Chem. Soc.* **1999**, *121*, 12200. (d) Yamashita, K.; Janout, V.; Bernard, E. M.; Armstrong, D.; Regen, S. L. *J. Am. Chem. Soc.* **1995**, *117*, 6249.
(3) For general reviews: (a) Gokel, G. W.; Murillo, O. *Acc. Chem. Res.* **1996**, *29*, 425. (b) Kobuke, Y. In *Advances in Supramolecular Chemistry*; Gokel, G. W., Ed.; JAI Press: Greenwich, CT, 1997; Vol. 4, pp 163−210. For recent examples: (c) Sakai, N.; Brennan, K. C.; Weiss, L. A.; Matile, S. *J. Am. Chem. Soc.* **1997**, *119*, 8726. (d) Weiss, L. A.; Sakai, N.; Ghebremariam, B.; Ni, C.; Matile, S. *J. Am. Chem. Soc.* **1997**, *119*, 12142. (e) Tedesco, M. M.; Ghebremariam, B.; Sakai, N.; Matile, S. *Angew. Chem., Int. Ed.* **1999**, *38*, 540. (f) Fyles, T. M.; Loock, D.; Zhou, X. *J. Am. Chem. Soc.* **1998**, *120*, 2997. (g) Abel, E.; Maguire, G. E. M.; Meadows, E. S.; Murillo, O.; Jin, T.; Gokel, G. W. *J. Am. Chem. Soc.* **1997**, *119*, 9061. (h) Abel, E.; Maguire, G. E. M.; Murillo, O.; Suzuki, I.; De Wall, S. L.; Gokel, G. W *J. Am. Chem. Soc.* **1999**, *121*, 9043. (i) Clark, T. A.; Buehler, L. K.; Ghadiri, M. R. *J. Am. Chem. Soc.* **1998**, *120*, 651. (j) Otto, S.; Osifchin, M.; Regen, S. L. *J. Am. Chem. Soc.* **1999**, *121*, 7276. (k) Baumeister, B.; Sakai, N.; Matile, S. *Angew. Chem., Int. Ed.* **2000**, *39*, 1955. (l) Schrey, A.; Vescovi, A.; Knoll, A.; Rickert, C.; Koert, U. *Angew. Chem., Int. Ed.* **2000**, *39*, 900. (m) Arndt, H.-D.; Knoll, A.; Koert, U. *Angew. Chem., Int. Ed.* **2001**, *40*, 2076. (n) Bandyopadhyay, P.; Janout, V.; Zhang, L.; Regen S. L. *J. Am. Chem. Soc.* **2001**, *123*, 7691. (o) Bandyopadhyay, P.; Janout, V.; Zhang, L.; Sawko, J, A.; Regen S. L. *J. Am. Chem. Soc.* **2000**, *122*, 12888. (p) Ishida, H.; Qi, Z.; Sokabe, M.; Donowaki, K.; Inoue, Y. *J. Org. Chem.* **2001**, *66*, 2978. (q) Gokel, G. W.; Ferdani, R.; Liu, J.; Pajewski, R.; Shabany, H.; Uetrecht, P. *Chem. Eur. J.* **2001**, *7*, 33. (r) Kobuke, Y.; Nagatani, T. *J. Org. Chem.* **2001**, *66*, 5094.

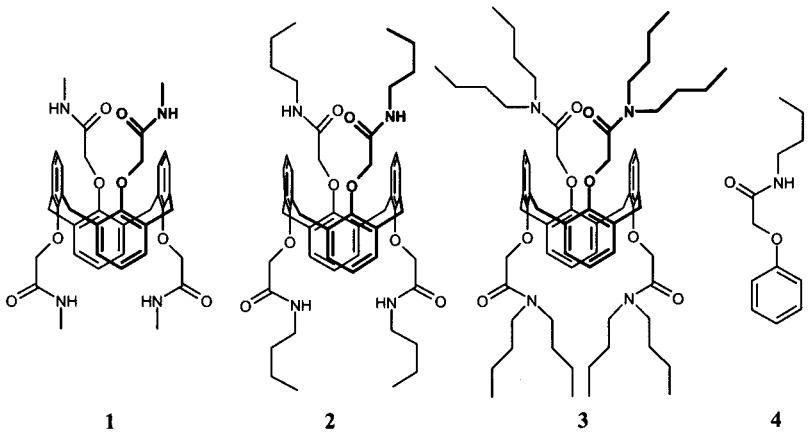

Figure 1. Compounds used in this study.

structures of the mechanosensitive ion channel and the K^+ channel.[8]

Expanding on the work of Shinkai[9] and Hosseini,[10] we recently used cation-templated self-assembly to build tubular constructs containing an ion-filled pore. Thus, a calix[4]arene *1,3-alt*[11] bearing four guanosine units formed micron-length rods in the presence of $NaBPh_4$.[12] This controlled aggregation was ascribed to the ability of Na^+ to stabilize a hydrogen-bonded G-quartet,[13] a motif that bridged calixarenes into a tubular structure. Calix[4]arenes are attractive scaffolds due to their ready preparation and functionalization,[11] their rigidity, and their ability to bind charged[14] and neutral species.[15] Of relevance are the findings that calix[4]arene-crown ethers[16] and calix[4]-resorcinarenes[17] form synthetic cation channels in lipid membranes.

While investigating self-assembly of our guanosine−calixarene conjugate,[12] we focused attention on the secondary amides that connect the nucleosides to the calix[4]arene *1,3-alt* scaffold. We prepared compounds **1**−**4** shown in Figure 1 to determine whether calix[4]arene *1,3-alt* amides might self-assemble in the presence of cations and/or anions. Herein, we report that calix[4]arene tetrabutylamide **2** binds HCl in solution, forms ion channels in a lipid bilayer, and effectively transports HCl across liposomal and cell membranes. We also present solid-state evidence that the analogous calix[4]arene tetramethylamide **1** self-assembles in the presence of HCl to form ordered arrays containing chloride-filled and water-filled channels. By comparing ion binding and transport properties of calix[4]arene tetrabutylamide **2** with those of its analogues **1**, **3**, and **4**, we find that the compound's hydrophobicity, the amide's substitution pattern, and the calixarene's macrocyclic framework are essential for mediating ion transport. The evidence points toward a self-assembled channel being formed by calix[4]arene tetrabutylamide **2** in an anion-dependent process.

Results and Discussion

Calix[4]arene tetramethylamide **1**,[12] tetrabutylamide **2**, and octabutylamide **3** were prepared by coupling the appropriate amine with calix[4]arene-*1,3-alt* tetraacid chloride.[12] Synthesis and characterization of **1**−**3** are detailed in the Experimental Section.

Calix[4]arene tetrabutylamide 2 transports ions across the bilayer without cation selectivity, whereas calix[4]arene tetramethylamide 1 does not mediate ion transport. The ability of **1** and **2** to mediate ion flux across a lipid bilayer was studied fluorimetrically (Figure 2). A solution of **1** or **2** was added to a suspension of EYPC large unilamellar vesicles (LUVs) containing the pH-sensitive dye pyranine.[18] A NaOH solution was added to the extravesicular buffer to create a gradient of approximately one pH unit. The resulting electrostatic potential, caused by proton efflux from the liposomes, can be compensated by cation influx or anion efflux, as mediated by the exogenous ligand.[19] Ion transport across the membrane was signaled by the increase in relative fluorescence that accompanied the rise in intravesicular pH.

(4) (a) Reddy, G. L.; Iwamoto, T.; Tomich, J. M.; Montal, M. *J. Biol. Chem.* **1993**, *268*, 14608. (b) Oblatt-Montal, M.; Reddy, G. L.; Iwamoto, T.; Tomich, J. M.; Montal, M. *Proc. Nat. Acad. Sci., U.S.A.* **1994**, *91*, 1495. (c) Wallace, D. P.; Tomich, J. M.; Eppler, J. W.; Iwamoto, T.; Grantham, J. J.; Sullivan, L. P. *Biochim. Biophys. Acta (Biomembranes)* **2000**, *1464*, 69. (d) Mitchell, K. E.; Iwamoto, T.; Tomich, J.; Freeman, L. C. *Biochim. Biophys. Acta (Biomembranes)* **2000**, *1466*, 47. (e) Broughman, J. R.; Mitchell, K. E.; Sedlacek, R. L.; Iwamoto, T.; Tomich, J. M.; Schultz, B. D. *Am. J. Physiol.: Cell Physiol.* **2001**, *280*, C451.

(5) (a) Deng, G.; Dewa, T.; Regen, S. L. *J. Am. Chem. Soc.* **1996**, *118*, 8975. (b) Merritt, M.; Lanier, M.; Deng, G.; Regen, S. L. *J. Am. Chem. Soc.* **1998**, *120*, 8494.

(6) Ashcroft, F. M. *Ion Channels and Disease*; Academic Press: New York, 2000; pp 186−198.

(7) Anderson M. P.; Sheppard, D. N.; Berger, H. A.; Welsh, M. J. *Am. J. Physiol.* **1992**, *263*, L1.

(8) (a) Chang, G.; Spencer, R. H.; Lee, A. T.; Barclay, M. T.; Rees, D. C. *Science* **1998**, *282*, 2220. (b) Doyle, D. A.; Cabral, J. M.; Pfuetzner, R. A.; Kuo, A. L.; Gulbis, J. M.; Cohen, S. L.; Chait, B. T.; MacKinnon, R. *Science* **1998**, *280*, 69.

(9) Ikeda, A.; Shinkai, S. *Chem. Commun.* **1994**, 2375.

(10) (a) Jaunky, W.; Hosseini, M. W.; Planeix, J. M.; De Cian, A.; Kyritsakas, N.; Fischer, J. *Chem. Commun.* **1999**, 2313. (b) Kleina, C.; Graf, E.; Hosseini, M. W.; De Cian, A.; Fischer, J. *Chem. Commun.* **2000**, 239.

(11) (a) Gutsche, C. D. Calixarenes. In *Monographs in Supramolecular Chemistry*; Stoddart, J. F., Ed.; Royal Society of Chemistry: Cambridge, 1989. (b) Gutsche, C. D. Calixarenes Revisited. In *Monographs in Supramolecular Chemistry*; Stoddart, J. F., Ed.; Royal Society of Chemistry: Cambridge, 1998.

(12) Sidorov, V.; Kotch, F. W.; El-Kouedi, M.; Davis, J. T. *Chem. Commun.* **2000**, 2369.

(13) (a) Guschlbauer, W.; Chantot, J. F.; Thiele, D. *J. Biomol. Struct. Dynam.* **1990**, *8*, 491 (b) Wong, A.; Fettinger, J. C.; Forman, S. F.; Davis, J. T.; Wu, G. *J. Am. Chem. Soc.* **2002**, *124*, 742−743.

(14) (a) Böhmer, V. *Angew Chem., Int. Ed. Engl.* **1995**, *34*, 713. (b) Beer, P. D.; Gale, P. A. *Angew. Chem., Int. Ed.* **2001**, *40*, 487.

(15) (a) Arduini, A.; McGregor, W. M.; Paganuzzi, D.; Pochini, A.; Secchi, A.; Ugozzoli, F.; Ungaro, R. *Perkin Trans. 2* **1996**, 839. (b) Smirnov, S.; Sidorov, V.; Pinkhassik, E.; Havlicek, J.; Stibor, I. *Supramol. Chem.* **1997**, *8*, 187.

(16) de Mendoza, J.; Cuevas, F.; Prados, P.; Meadows, E. S.; Gokel, G. W. *Angew. Chem., Int. Ed.* **1998**, *37*, 1534.

(17) (a) Yoshino, N.; Satake, A.; Kobuke, Y. *Angew. Chem., Int. Ed.* **2001**, *40*, 457. (b) Tanaka, Y.; Kobuke, Y.; Sokabe, M. *Angew. Chem., Int. Ed.* **1995**, *34*, 693. (c) Wright, A. J.; Matthews, S. E.; Fischer, W. D.; Beer, P. D. *Chem. Eur. J.* **2001**, *7*, 3474.

(18) Kano, K.; Fendler, J. H. *Biochim. Biophys. Acta* **1978**, *509*, 289.

(19) For more on the pH-gradient transport assays see refs 3c−e.

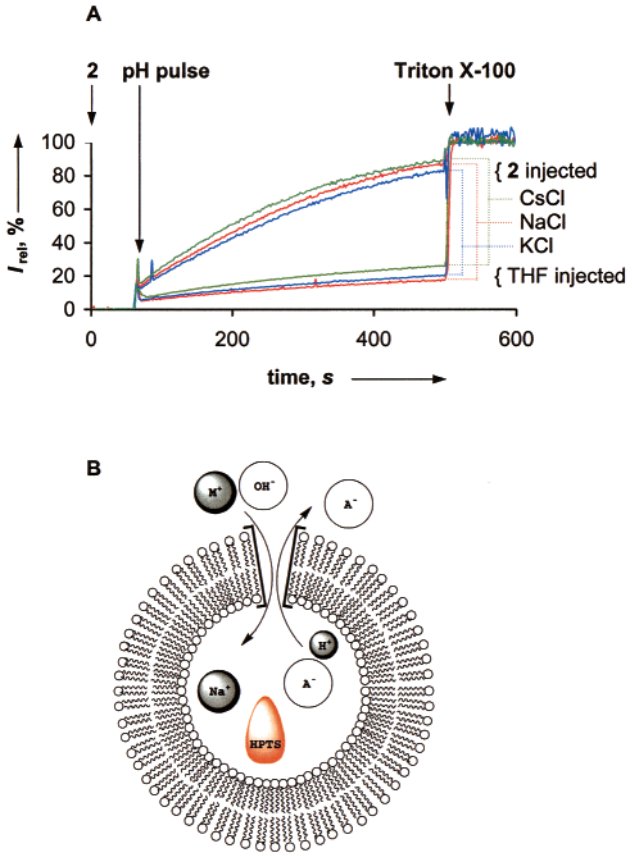

Figure 2. (A) Liposome transport assays with **2** in the presence of NaCl, KCl, and CsCl. Suspensions of EYPC LUVs containing the pH-sensitive dye pyranine in a phosphate buffer were used. The intravesicular solution contained 10 mM sodium phosphate, pH 6.4, 100 mM NaCl and the extravesicular solution contained 10 mM sodium phosphate, pH 6.4, 100 mM MCl (M = Na, K, Cs). At t = 0 s, 20 μL of a 0.5 mM solution of **2** in THF was added (top three curves) to give 1:100 **2**:lipid molar ratio or 20 μL of THF was added (bottom three curves). At t = 60 s, 21 μL of a 0.5 M NaOH solution was added. At t = 500 s, 40 μL of 5% Triton X-100 was added. Counting from top to bottom, traces 1 and 4 correspond to the solutions containing 100 mM CsCl, traces 2 and 6 correspond to the solutions containing 100 mM NaCl, and traces 3 and 5 correspond to solutions containing 100 mM KCl buffer. (B) Schematic representation of transport experiments. A pH gradient results from addition of extravesicular NaOH solution. The charge caused by H^+ efflux or OH^- influx is compensated by cation influx or anion efflux, as mediated by the exogenous ligand such as **2**. The increase in intravesicular pH, monitored by the entrapped pH-sensitive dye, HPTS, reflects the electrolyte exchange rate.

The polyanionic pyranine is known to adsorb strongly to positively charged vesicles.[18,20,21] Pyranine also adsorbs to some extent to neutral liposomes such as EYPC.[5b] Our fluorescence traces, which measure the ratio of deprotonated to protonated forms of the dye (see Experimental Section), register a response that is directly proportional to pH.[22] In this way, dye adsorption to the internal surface of the vesicles does not interfere with the pH measurements. We can estimate the amount of dye adsorbed to the outer surface of EYPC LUVs by analyzing the burst response upon base addition (Figure 2a). This response has never exceeded 15% of the total fluorescence change observed in the course of the experiments. The slower phase of fluorescence increase is due to the rise in intravesicular pH as calixarene **2** transports ions across the EYPC membrane. It is the rate constant for this second phase that we report in Table 1. Furthermore, negative controls shown in Figure 2 clearly indicate that there is little fluorescence increase in the absence of calixarene **2**.

Table 1. Initial Pseudo-first Order Transport Rate Constants ($\times 10^{-3}$ s^{-1}) for Intravesicular and Extravesicular Electrolyte Exchange in the Presence of 5 μM of **2** or **3** and Different Salts

salt transporter	NaCl	KCl	CsCl	Na_2SO_4
2[a]	6.8[b,c]	6.4[b,c]	7.7[b,c]	1.1[b,d]
3[a]	19[b,c]	12[b,c]	5.4[b,c]	9.1[b,d]

[a] 20 μL of 0.5 mM THF solution of the compound was added to 2 mL of a 0.5 mM LUV suspension. [b] Rate constants were determined as described in the Experimental Section. Values are not corrected for unmediated electrolyte exchange. The accuracy of measurements was ±15% for experiments using the same set of liposomes. [c] 100 mM NaCl, 10 mM phosphate buffer, pH 6.4 inside; 100 mM MCl, M = Na, K, or Cs, 10 mM phosphate buffer, pH 7.4 outside, after pH pulse. Note that values are not directly comparable because of different ion gradients. [d] 100 mM Na_2SO_4, 10 mM phosphate buffer, pH 6.4 inside; 100 mM Na_2SO_4, 10 mM phosphate buffer, pH 7.4 outside, after pH pulse.

Calix[4]arene tetramethylamide **1** showed little transport activity in the presence of extravesicular Na^+, K^+, or Cs^+ chloride at ligand:lipid ratios of up to 1:20,[23] whereas rapid exchange of intra- and extravesicular electrolytes was observed in the presence of calix[4]arene tetrabutylamide **2** at a ligand:lipid ratio of 1:100 (Figure 2a). These fluorescence assays in buffers containing Na^+, K^+, or Cs^+ indicated that ion transport mediated by **2** was nonselective toward the cation (Figure 2a, Table 1). The reduced activity for tetramethylamide **1** can be attributed to its lower hydrophobicity with respect to tetrabutylamide **2**.[24]

Calix[4]arene tetrabutylamide 2 does not induce defects into the bilayer membrane but provides selective transport of Cl^- over HSO_4^-. Calix[4]arene tetrabutylamide **2** may transport ions across LUVs by inducing membrane defects, by uniport of ions, or via cotransport of ion pairs (H^+/M^+ or OH^-/A^- antiport and H^+/A^- or M^+/OH^- symport mechanisms are possible). The lytic potential of **2** was evaluated using a dye release assay. The self-quenching dye calcein loses 95% of its fluorescence emission at concentrations above 100 mM.[25] A suspension of LUVs containing 120 mM calcein showed no fluorescence enhancement upon dilution with an isoosmotic buffer containing **2** (5−100 μM, 1−20 mol % ligand, relative to total lipid concentration, data not shown). This calcein experiment indicates that **2** does not induce membrane defects.

Secondary amides can interact with anions and cations, making it reasonable that calix[4]arene tetrabutylamide **2** could

(20) Clement, N. R.; Gould, J. M. *Biochemistry* **1981**, *20*, 1534.
(21) Dye adsorption can be minimized by incorporation of negatively charged lipids into the liposomes. Such liposomes discriminate, however, in their membrane permeability toward different monovalent cations (Papahadjopoulos, D. *Biochim. Biophys. Acta* **1971**, *241*, 254) and, therefore, may cause misleading results in our transport assays.
(22) Venema, K.; Gibrat, R.; Grouzis, J.-P.; Grignon, C. *Biochim. Biophys. Acta* **1993**, *1146*, 87.
(23) Initial pseudo-first-order rate constants determined for NaCl, KCl, and CsCl in the presence of 25 μM of **1** were 2.5, 2.2, and 4.1 ($\times$ 10^{-3} s^{-1}), respectively (ligand: lipid ratio 1:20). Rate constants in the absence of **1** or **2** were in the range of 1.5−2.7 ($\times$ 10^{-3} s^{-1}) for all three salts. No transport was observed in the presence of 5 μM of **1**(ligand:lipid ratio 1:100).
(24) The relative hydrophobicity of **1** and **2** was clearly different based on reverse phase HPLC retention times (C-18, 1:1 CH_3CN:0.1% aqueous TFA, flow rate of 1 mL/min). Retention times were 4.8 and 54.1 min for **1** and **2**, respectively. For use of RPLC retention times as a measure of partition coefficients: Kaliszan, R. in *Quantitative Structure−Chromatographic Retention Relationships.* **1987**. pp 232−267, John Wiley & Sons: New York.
(25) New, R. R. C. in *Liposomes: a Practical Approach*; IRL Press: Oxford, 1990; pp 131−134.

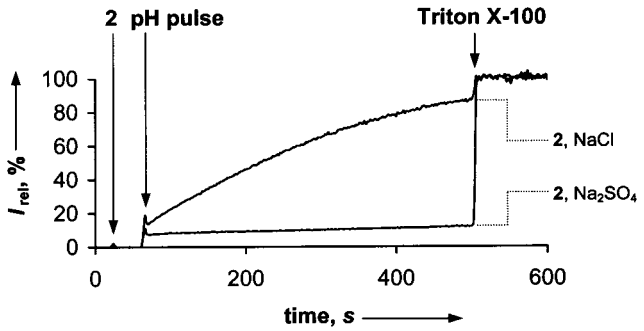

Figure 3. Transport assays with **2** in the presence of extravesicular buffers containing NaCl (top trace) and Na_2SO_4 (lower trace). Suspensions of EYPC LUVs containing the pH-sensitive dye pyranine in a phosphate buffer were used. At t = 20 s, 20 μL of a 500 μM of **2** in THF was added to 1.95 mL of LUV suspension to give 1:100 **2**:lipid molar ratio. At t = 60 s, 21 μL of 0.5 M NaOH was added to change the extravesicular pH from 6.4 to 7.4. At t = 500 s, 40 μL of 5% Triton X-100 was added. No significant transport in the Na_2SO_4 buffer was observed even in the presence of up to 50 μM of **2**.

transport either ion type. Since the transport activity of calix[4]arene **2** was cation-independent (Figure 2a), we tested whether ion transport mediated by **2** might be anion dependent. Standard fluorescence assays were conducted with sodium sulfate-filled LUVs suspended in an isotonic solution. Unlike for chloride-containing solutions, experiments in sulfate buffers revealed that the pH-induced ion flux across the membrane was not mediated by 5−50 μM concentrations of **2** (1−10 mol % ligand, Figure 3). This pronounced Cl^-/HSO_4^- transport selectivity (Table 1) implies that **2** functions as a Cl^- transporter.

^{1}H NMR experiments show that calix[4]arene tetrabutylamide 2 binds HCl. To obtain evidence for Cl^- binding by **2**, we carried out ^{1}H NMR experiments in $CDCl_3$ using n-Bu_4NCl and HCl as Cl^- sources (Figure 4). Anion receptors usually show chemical shift perturbations upon anion complexation, particularly for amide NH protons that hydrogen bond to the anion.[26] Surprisingly, no changes in the ^{1}H NMR spectrum of the secondary amide **2** in $CDCl_3$ were observed upon addition of n-Bu_4NCl (Figure 4b). This lack of spectral changes indicates that **2** does not bind strongly to the "naked" Cl^- anion, even in this nonpolar solvent. Calix[4]arene tetrabutylamide **2** does, however, bind HCl. Thus, shaking a $CDCl_3$ solution of **2** with aqueous HCl led to disappearance of the amide NH proton and a significant upfield shift of the O*CH*$_2$C(O) protons (Figure 4c). The NMR spectral changes of **2** induced by HCl extraction were not simply due to acid treatment, since washing a $CDCl_3$ solution of **2** with a H_2SO_4 solution did not cause any changes (Figure 4d).

These ^{1}H NMR experiments indicate that calix[4]arene tetrabutylamide **2** is a ditopic HCl receptor, since both H^+ and Cl^- are needed to induce spectral changes. These NMR data for **2** are consistent with the LUV transport results, where efficient ion transport across the membrane was observed in the presence of Cl^- but not HSO_4^-. The combined fluorescence and NMR results lead us to conclude that calix[4]arene tetrabutylamide **2** supports ion transport across LUVs in an anion-dependent fashion by either an H^+/Cl^- symport or a Cl^-/OH^- antiport mechanism.[27]

Calix[4]arene tetrabutylamide 2 mediates effective H^+/Cl^- transport across bilayer membranes. With NMR evidence that calix[4]arene tetrabutylamide **2** binds HCl in a hydrophobic environment we asked whether **2** could transport HCl across LUVs. Previously, we showed that a pH gradient across Cl^--filled vesicles was collapsed by addition of **2** (Figure 2a). We studied the reverse situation by monitoring the intravesicular pH of LUVs experiencing a Cl^- gradient (Figure 5).

When a suspension of LUVs filled with saline phosphate buffer (100 mM NaCl, 10 mM sodium phosphate, pH 6.4) and suspended in isoosmotic Na_2SO_4 buffer (75 mM Na_2SO_4, 10 mM sodium phosphate, pH 6.4) was treated with **2**, we observed a rapid increase in intravesicular pH (Figure 5, top trace). The pH reached its maximum ~250 *s* after addition of **2** and held constant until the liposomes were lyzed with detergent.[28,29] These results are consistent with an H^+/Cl^- symport or Cl^-/OH^- antiport process. In effect, compound **2** moves H^+ along with Cl^- down the chloride gradient, consequently building a pH gradient across the membrane. Therefore, NaCl-filled vesicles lose Cl^- and H^+ upon addition of **2** and become more alkaline.[30,31]

The secondary amide NH and calix[4]arene framework are essential for the HCl transport activity of 2. Calix[4]arene octabutylamide **3** was used as a negative control for tetrabutylamide **2**, as the lack of amide NH protons in **3** would preclude Cl^- binding. Instead, **3** should be a cation ionophore, much like tetrakis(diethylcarbamoylmethoxy)-*p-tert*-butylcalix[4]arene-*1,3-alt* that coordinates cations in the solid-state and solution.[32] To confirm that **3** binds Na^+, sodium picrate extraction in $CDCl_3$ was monitored by ^{1}H NMR spectroscopy. Complexation of the salt by **3** was evident. Two distinct complexes were formed, corresponding to a 1:1 and a 2:1 Na^+:**3** stoichiometry (Figure 6). The 1:1 complex was generated by adding 1 equiv of solid sodium picrate to a solution of **3**. Binding

(26) (a) Kavallieratos, K.; Bertao, C. M.; Crabtree, R. H. *J. Org. Chem.* **1999**, *64*, 1675. (b) Deetz, M. J.; Shang, M.; Smith, B. D. *J. Am. Chem. Soc.* **2000**, *122*, 6201.

(27) Attempts to distinguish H^+/Cl^- symport and Cl^-/OH^- antiport mechanisms by carrying out transport assays on polarized vesicles failed. Electrical silence of transport is usually ascribed to a symport mechanism. Electrical current leading to a change in membrane potential is, however, possible for both symport and antiport mechanisms. Although no apparent alteration of transport rates due to the membrane potential was observed in the presence of **2**, monitoring the membrane potential revealed its rapid collapse upon application of **2**. Further transport occurred across the nonpolarized membrane. Moreover, injection of **2** into a suspension of vesicles experiencing a Cl^- gradient (Na_2SO_4 inside, NaCl outside) resulted in a potential with the negative pole inside the membrane. Apparently, H^+ and Cl^- transport occur at different rates.

(28) A base-pulse assisted transport assay carried out on unequally loaded vesicles (NaCl inside, Na_2SO_4 outside) revealed a ~165% transport rate, as judged from lysis of liposomes by Triton X-100.

(29) Formation of a pH gradient across the membrane arising from ionophore-mediated Cl^-/OH^- exchange has been reported for Hg^{2+} and Cu^+ salts: (a) Karniski, L. P. *J. Biol. Chem.* **1992**, *267*, 19218, organotin, organolead, and organomercury compounds: (b) Watling, A. S.; Selwyn, M. J. *FEBS Lett.* **1970**, *10*, 139, (c) Selwyn, M. J.; Dawson, A. P.; Stockdale, M.; Gains, N. *Eur. J. Biochem.* **1970**, *14*, 120. (d) Wieth, J. O.; Tosteson, M. T. *J. Gen. Physiol.* **1979**, *73*, 765, and prodigiosins: (e) Sato, T.; Konno, H.; Tanaka, Y.; Kataoka, T.; Nagai, K.; Wasserman, H. H.; Ohkuma, S. *J. Biol. Chem.* **1998**, *273*, 21455.

(30) The proton regulatory function displayed by **2** is similar to that of the anion-exchanging protein's function in red blood cells: Jennings, M. L. *J. Membr. Biol.* **1978**, *40*, 365.

(31) Preliminary experiments on inversely loaded vesicles (Na_2SO_4 inside, NaCl outside, HPTS as dye) revealed acidification of the vesicular compartment upon addition of **2**. This result is qualitatively consistent with HCl influx. The pH change for these inversely loaded vesicles was, however, lower than that observed for NaCl-filled vesicles suspended in sulfate buffer (Figure 5, top trace). This nonsymmetrical response in the two experiments may be due to changes in osmotic pressure during the experiment or due to Cl^--mediated aggregation of **2** in the saline buffer. Such possibilities will be investigated as part of our ongoing study.

(32) Beer, P. D., Drew, M. G. B.; Gale, P. A.; Leeson, P. B.; Odgen, M. I. *J. Chem. Soc., Dalton Trans.* **1994**, 3479.

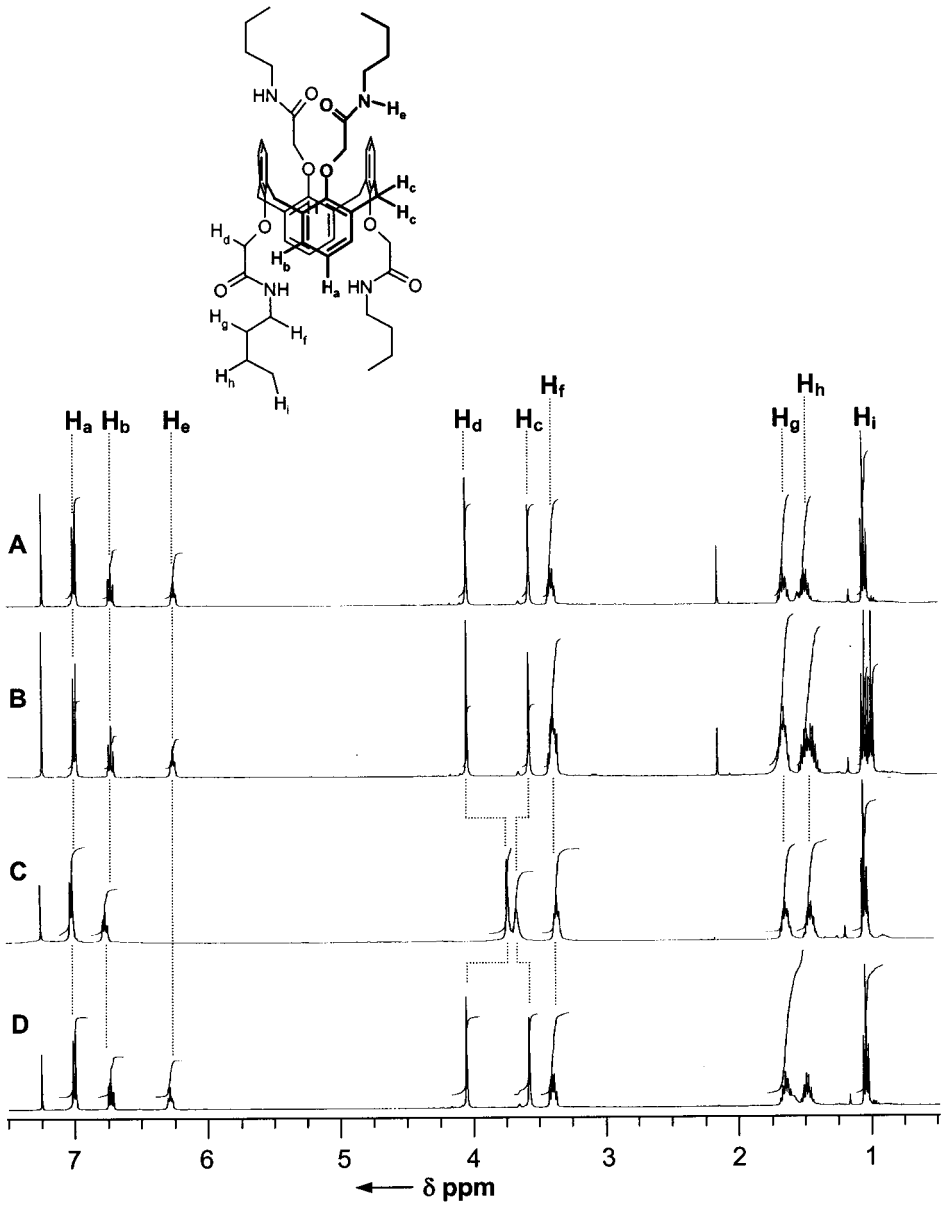

Figure 4. A series of ^{1}H NMR spectra (400 MHz, $CDCl_3$, 22 °C) of calixarene tetrabutylamide **2** in the presence of different species: (A) compound **2** alone (5 mM); (B) **2** with 1 equiv of Bu_4NCl; (C) after washing $CDCl_3$ solution of **2** with aqueous solution of 0.5 M HCl; (D) after washing $CDCl_3$ solution of **2** with aqueous solution of 0.5 M H_2SO_4.

this Na^+ led to a symmetry loss for **3**, indicated by doubling of the ^{1}H NMR peaks. Addition of further sodium picrate (up to 10 equiv) resulted in a new 2:1 complex. Binding of the second Na^+ cation restored the ligand's initial D_{2d} symmetry, as seen by the new set of single NMR signals for this 2:1 complex.[32] In contrast, sodium picrate extraction by calix[4]arene tetrabutylamide **2** was not detected by ^{1}H NMR spectroscopy.

Ion transport assays revealed a high activity for octabutylamide **3** in NaCl buffer ($k = 1.9 \times 10^{-2}$ s^{-1}, Table 1). Unlike **2**, calix[4]arene octabutylamide **3** discriminates between monovalent cations, showing a 3.5-fold drop in rate constant when changing the extravesicular electrolyte from NaCl to CsCl (Table 1). Fluorescence assays with **3** in the presence of Na_2SO_4 loaded vesicles suspended in isotonic buffer indicated that **3** still mediated significant ion transport, albeit with a drop in activity ($k = 9.1 \times 10^{-3}$ s^{-1}). In marked contrast, calix[4]arene tetrabutylamide **2** had shown essentially complete loss of transport activity when the buffer was changed from one containing NaCl to one containing Na_2SO_4 (Figure 3, Table 1).[33] Further evidence for different ion transport selectivity provided by calixarene octabutylamide **3** and tetrabutylamide **2** was obtained from an experiment with NaCl-loaded vesicles suspended in isoosmotic Na_2SO_4 solution. Addition of **3** did not result in formation of a pH gradient across the membrane (Figure 5, bottom trace), whereas addition of **2** to the identical system had produced a significant pH gradient (Figure 5, top trace).

To determine whether chloride binding and transport is an intrinsic property of calixarene **2** or a general property of hydrophobic secondary amides, *N*-butyl-2-phenoxyacetamide **4** (Figure 1) was tested in the LUV transport assays. Compound **4** is a monomeric analogue of calixarene **2**, bearing a secondary amide that could bind Cl^-, but lacking the calixarene's macrocycle. The standard fluorescence assay, even in the

(33) The initial pseudo-first-order rate constant changed from 7.9 to 1.1 ($\times 10^{-3}$ s^{-1}) for 5 μM of **2** when changing from a Cl^- to SO_4^{2-} buffer. The latter value is indistinguishable from the rate constant in the absence of **2**.

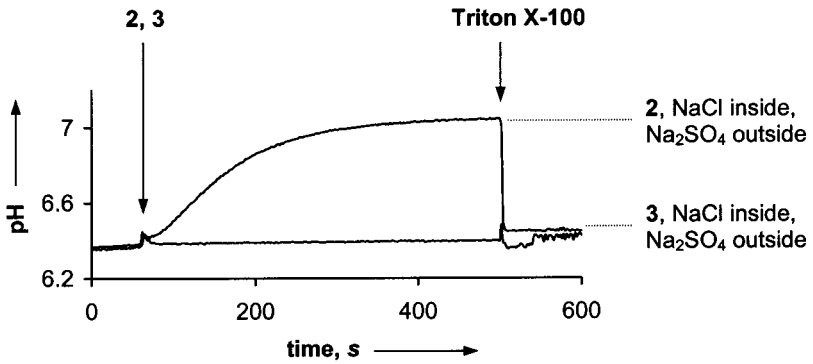

Figure 5. Changes in intravesicular pH upon addition of calixarene tetrabutylamide **2** and calixarene octabutylamide **3** to NaCl-loaded vesicles suspended in a sulfate phosphate buffer (emission of HPTS is used to monitor the pH changes in LUV's). At t = 60 s, 20 μL of 500 μM of **2** (top trace) or **3** (bottom trace) was added to 1.95 mL of a LUV suspension to give 1:100 ligand:lipid molar ratio. At t = 500 s, 40 μL of 5% Triton X-100 was added. Intravesicular pH values were obtained as a function of the ratio of HPTS emission intensities at 510 nm, when excited at 403 and 460 nm. The calibration was performed by measuring the HPTS emission intensities and the pH values of a 4.70 nM HPTS solution in 10 mM phosphate buffer containing 100 mM NaCl. The calibration equation obtained (pH = $1.1684 \times \log(I_o/I_1) + 6.9807$, $r = 0.998$, where I_o is the emission intensity with excitation at 460 nm and I_1 is emission intensity with excitation at 403 nm) was used to convert the emission intensities into actual pH values.

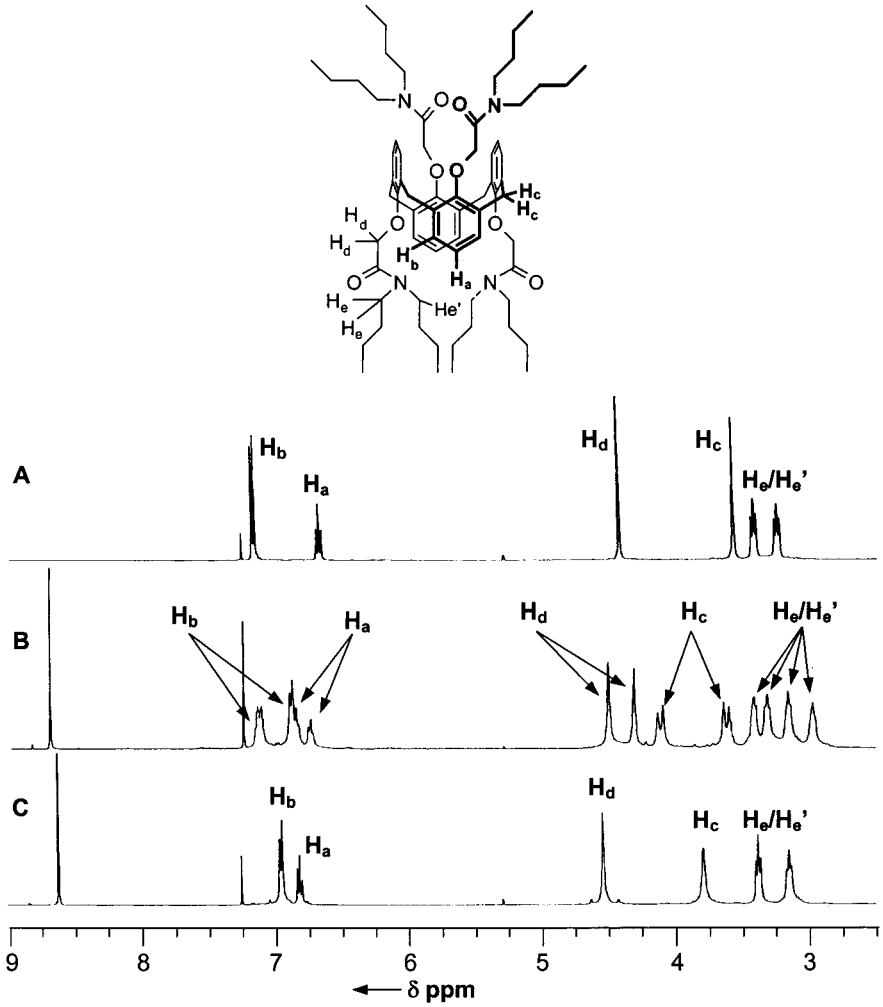

Figure 6. (A) Region of the ^{1}H NMR spectrum (400 MHz, $CDCl_3$, 22 °C) of calixarene octabutylamide **3** (5 mM) in $CDCl_3$, (B) compound **3** after addition of 1 equiv of NaPic, (C) compound **3** after addition of 2 equiv of NaPic. No change in this NMR spectrum was observed in the presence of up to 10 equiv of solid NaPic.

presence of high concentrations of **4** (50 μM) showed no ion transport across the LUV membrane. In addition, ^{1}H NMR spectroscopy indicated no HCl binding by **4** in $CDCl_3$. These controls with *N*-butyl-2-phenoxyacetamide **4** support the hypothesis that the calixarene's core is critical for the HCl binding and ion transport properties of **2**.

Calix[4]arene tetramethylamide 1 and HCl form channels in the solid state. After failing to crystallize tetrabutylamide **2**, we turned attention to the analogous calix[4]arene tetramethylamide **1**. Whereas **1** does not transport ions efficiently across the LUV membrane, presumably due to insufficient hydrophobicity, its mode of HCl binding should be similar to

Table 2. Crystal Data and Structure Refinement for **1**·HCl·3(H_2O) and **1**·HCl·H_2O·CH_2Cl_2 Complexes

	1·HCl·3(H_2O)	**1**·HCl·H_2O·CH_2Cl_2
empirical formula	$C_{40}H_{51}ClN_4O_{11}$	$C_{41}H_{49}Cl_3N_4O_9$
formula weight	799.29	848.18
temperature	193(2) K	193(2) K
crystal system	orthorhombic	monoclinic
space group	*Fddd*	*P*2(1)/*n*
unit cell dimensions	a = 20.9026(7) Å, α= 90°	a = 10.1237(3) Å, α= 90°
	b = 26.5756(9) Å, *β*= 90°	b = 22.7400(7) Å, *β*= 97.07°
	c = 27.7713(10) Å, *γ* = 90°	c = 17.7902(6) Å, *γ* = 90°
volume	15426.9(9) Å^3	4064.4(2) Å^3
Z	16	4
density (calculated)	1.375 mg/m^3	1.384 mg/m^3
absorption coefficient	0.166 mm^{-1}	0.286 mm^{-1}
data/restraints/parameters	3404/3/326	7147/0/723
goodness-of-fit on F_2	1.060	1.092
final *R* indices [$I > 2\sigma(I)$]	R1 = 0.0617, wR2 = 0.1785	R1 = 0.0431, wR2 = 0.1117
R indices (all data)	R1 = 0.0851, wR2 = 0.1958	R1 = 0.0570, wR2 = 0.1196

that for **2**. Different protocols afforded two types of **1**·HCl single crystals whose structures were solved by X-ray crystallography (see Table 2 for data). Both solid-state structures unequivocally show that Cl^- anion is hydrogen bonded to the calixarene's amide NH.

Crystals of **1**·HCl·3(H_2O), obtained by evaporation of a dichloromethane/THF solution of **1** and HCl, have a structure that consists of two-dimensional planar arrays of calixarenes held together by NH···Cl^-···HN hydrogen bonds in the x-direction and by C═O···H−O−H···O═C hydrogen bonds in the *y*-direction (Figure 7). A side view in the *y*-direction reveals a chloride-filled channel, and a side view in the *x*-direction reveals a water-filled channel.

Analysis of a second crystal (**1**·HCl·H_2O·CH_2Cl_2), grown by layering aqueous HCl over a dichloromethane solution of **1**, revealed a structure where two molecules of calixarene **1** are linked by oppositely directed N···Cl^-···H−O(H)$^+$−H···O═C bridges to give a dimer (Figure 8). Each molecule of calixarene **1** in **1**·HCl·H_2O·CH_2Cl_2 retains a similar geometry as observed in the structure of **1**·HCl·3(H_2O). The main difference in the second structure is that a hydronium cation separates Cl^- from the neighboring calixarene.

Although the three-dimensional network formed by the two **1**·HCl complexes is different, both crystal structures indicate that calixarene **1** uses its secondary amide groups to bind HCl. These crystal structures are relevant since they indicate that calix[4]arene *1,3-alt* amides can self-assemble to give extended channels held together by hydrogen bonds to bridging Cl^- anions and water.

Calix[4]arene tetrabutylamide 2 forms an ion channel. Ligand-mediated ion transport across a lipid bilayer is usually attributed to three mechanisms; defect induction, a carrier process, or channel formation.[3d,34] Dye-release experiments showed that **2** does not induce membrane defects. Both carrier and ion channel mechanisms for H^+/Cl^- transport are conceivable for a ligand like calix[4]arene tetrabutylamide **2**. A single molecule of **2** is certainly too small to span the membrane. But the calixarene's *1,3-alt* conformation makes channel-like structures possible, particularly in the presence of a bridging species. Crystal structures of the **1**·HCl complexes show calixarenes held together by amide···chloride···amide, amide···water···amide, and amide···chloride···water···amide hydrogen bonds. If HCl-mediated self-assembly of **2** gives similar structures in lipid membranes then such aggregates could act as ion channels. Even the shortest hydrogen-bonded unit in these structures, a calixarene dimer of ∼25 Å (Figure 8), could conceivably span a bilayer membrane.[35,36]

Since ion transport supported by **2** is not electrically silent,[27] current across the bilayer can be detected using the voltage-clamp technique, a technique that distinguishes between channel and carrier mechanisms. Evidence for ion channels formed by calix[4]arene tetrabutylamide **2** was obtained from voltage-clamp experiments on black lipid membranes (BLMs) (Figure 9).

The voltage-clamp assay was conducted using a setup with two chambers, each filled with an electrolyte solution and separated by a BLM. After voltage was applied across the membrane, a solution of **2** was added to one of the chambers. Subsequent current across the membrane was attributed to ion transport mediated by **2**, since control experiments with DMSO solvent were negative. Typical current recordings are shown in Figure 9a. The abrupt changes in current intensity (events) are consistent with an ion channel mechanism. The relatively long-lasting open states indicate that channels formed by calixarene tetrabutylamide **2** are stable.

Analysis of 480 events gave a distribution of conductance levels (50 pS-2 nS) centered near 100 pS (Figure 9b). We attribute the various conductivity levels to formation of different self-assembled channel structures.[37] One explanation for different assemblies formed by **2** is competition of calix[4]arene amides with water for Cl^- binding, as revealed in the two different crystal structures for **1**·HCl complexes (Figures 7 and 8). While one can only speculate about the structure of the active species, the experiments summarized in Figure 9 clearly indicate that calixarene **2** can form ion channels.

Calix[4]arene tetrabutylamide 2 forms voltage-dependent channels in HEK-293 cell membranes. Patch-clamp recordings in a whole-cell configuration (Figure 10a) revealed that extracellular application of **2** to HEK-293 cells caused current across

(34) Bell, T. W. *Curr. Opin. Chem. Biol.* **1998**, *2*, 711.

(35) (a) Caffrey, M.; Feigenson, G. W. *Biochem*istry **1981**, *20*, 1949. (b) Lewis, B. A.; Engelman, D. M. *J. Mol. Biol.* **1983**, *166*, 211.

(36) The active gramicidin dimer was estimated to have a length of 22 Å: (a) Ketchem, R. R.; Hu, W.; Cross, T. A. *Science* **1993**, *261*, 1457. (b) Goulian, M.; Mesquita, O. N.; Fygenson, D. K.; Nielsen, C.; Andersen, O. S.; Libchaber, A. *Biophys. J.* **1998**, *74*, 328.

(37) (a) Renkes, T.; Schafer, H. J.; Siemens, P. M.; Neumann, E. *Angew. Chem., Int. Ed.* **2000**, *39*, 2512. (b) Fyles, T. M.; Knoy, R.; Mullen, K.; Sieffert, M. *Langmuir* **2001**, *17*, 6669.

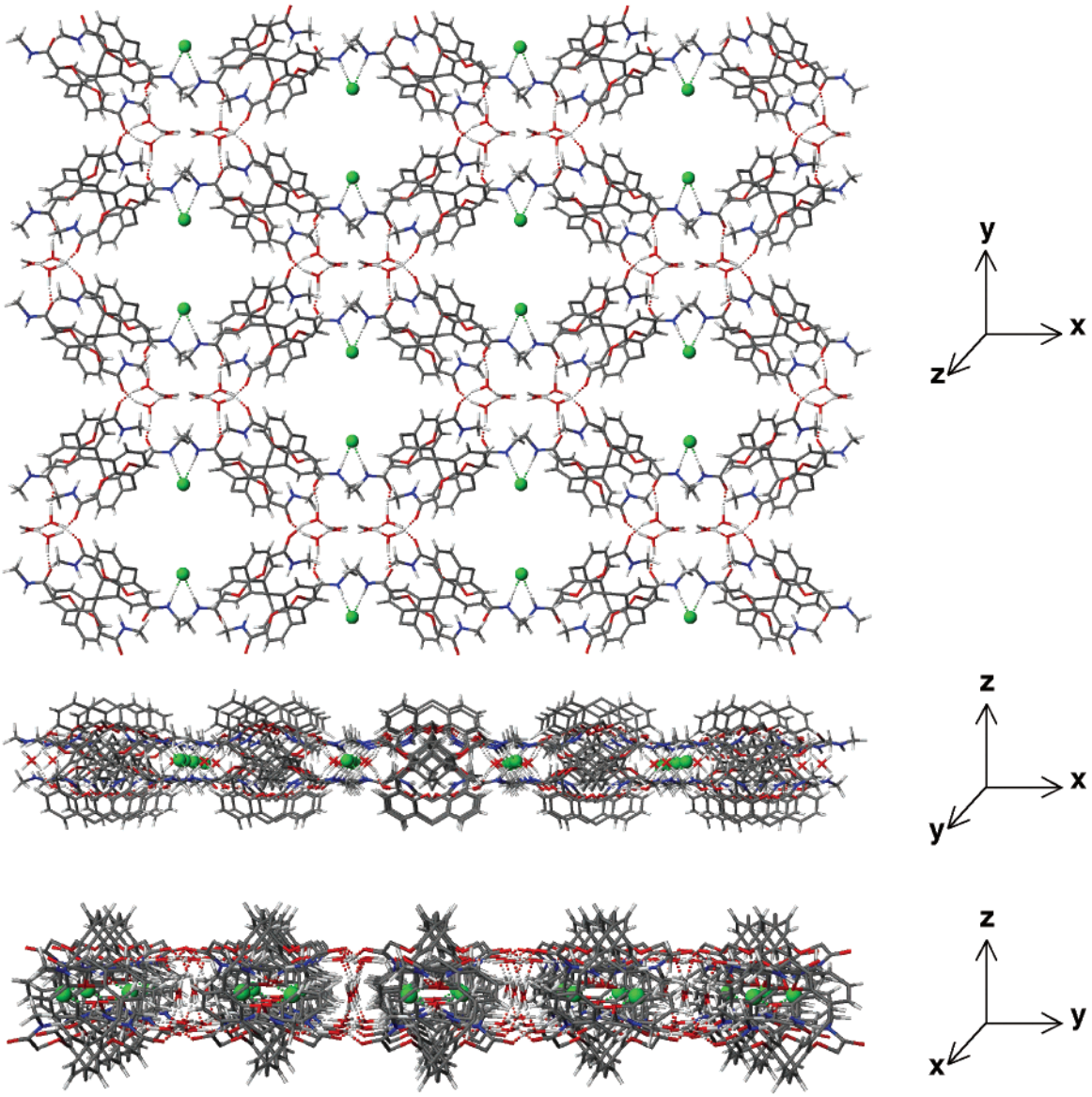

Figure 7. Top and side views of the hydrogen-bonded array found in the crystal structure of **1**·HCl·3(H_2O). The layer continues in the *x* and *y* directions infinitely. The *z*-direction is composed of identical layers held together by crystal-packing forces. The Cl^- anions are shown as green spheres. All molecules in the structure are shown in a wire frame representation following the standard color scheme. Hydrogen bonds between the water molecules depicted as tetrahedral (due to oscillation between two different binding modes) are omitted for clarity.

the cell membrane at holding potentials of +120 mV (3 of 15 cells actually responded at +80 mV, whereas the other cells responded at +120 mV). Importantly, this current was observed only when the cells were suspended in NaCl buffer. Replacement of NaCl buffer with isoosmotic Na glutamate (Figure 10b) or Na_2SO_4 (Figure 10c) resulted in no current across the membrane at holding potentials between −120 and +120 mV. These results lend further credence to the Cl^--selectivity of ion channels formed from calix[4]arene tetrabutylamide **2**.

Calixarene tetrabutylamide **2** could be washed out from the cell membrane. After 1.5 min of lavage, the current returned to the baseline (data not shown) and no further response at +120 mV was observed without further addition of **2**. These data indicate that application of **2** did not damage the cell membrane. Subsequent reapplication of **2** resulted in a shortening of the delay prior to the response (Figure 10d). One explanation for this phenomenon is that washing did not completely remove **2** from the cell membrane. Instead, inactive aggregates of **2** may remain. These membrane-retained "seeds" may then accelerate formation of new ion channels upon reapplication of the compound.

Conclusions

Calix[4]arene *1,3-alt* tetrabutylamide **2** binds HCl and forms ion channels in lipid bilayer membranes. This is a rare example of a synthetic, non-peptide ion channel showing an anion dependence. We attribute the HCl binding and transport activity of **2** to the calixarene's three-dimensional structure, its hydrophobicity and the amide side chain's substitution pattern. Alteration of any of these features results in a selectivity switch from anions to cations (compound **3**) or to loss of transport activity (compounds **1** and **4**). Ion transport provided by **2** proceeds via either an H^+/Cl^- symport or a Cl^-/OH^- antiport mechanism. Compound **2** can regulate H^+ and Cl^- gradients across the membrane. Two crystal structures demonstrate that the calix[4]arene *1,3-alt* tetraamide motif is capable of forming

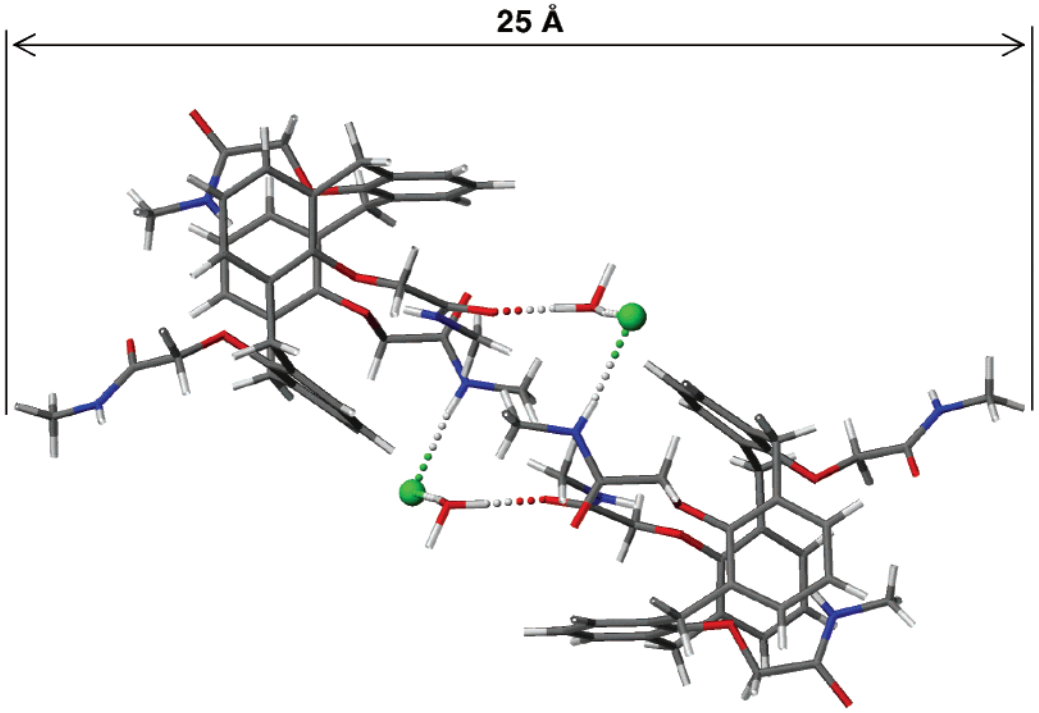

Figure 8. Self-assembled dimer observed within the **1**·HCl·H_2O·CH_2Cl_2 crystal structure. The CH_2Cl_2 molecules are omitted. The Cl^- anions are shown as green spheres. All molecules in the structure are shown in a wire frame representation following the standard color scheme.

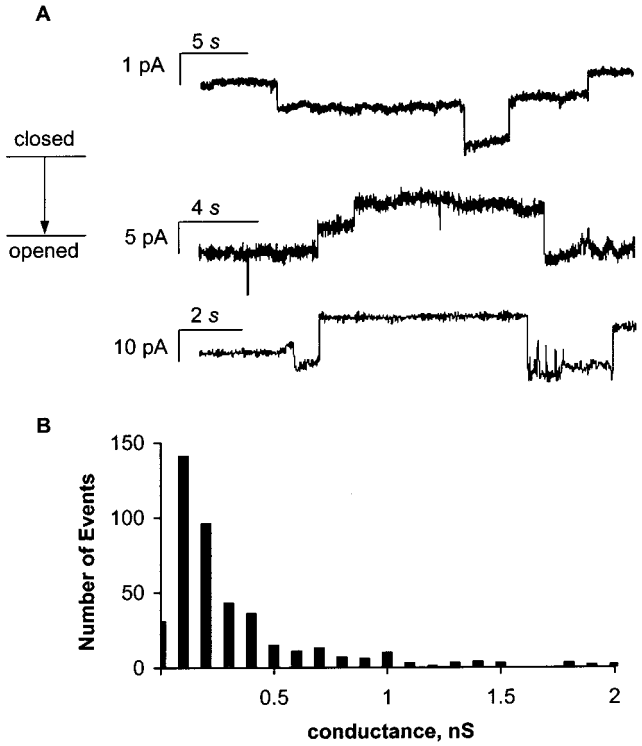

Figure 9. (A) Representative current events across a BLM in voltage clamp experiments after application of calixarene tetrabutylamide **2** (2.5 μM). The voltage applied was −20 mV for all three recordings. (B) The distribution of conductance ranges observed in voltage clamp experiments with **2** acting as an ion channel.

self-assembled channels filled with Cl^- anions and water. Finally, compound **2** enables Cl^--selective and voltage-dependent ion transport across HEK-293 cell membranes. This last property makes calix[4]arene *1,3-alt* tetrabutylamide **2** a potential antibiotic, capable of selective interactions with bacteria.[38]

Experimental Section

^{1}H NMR spectra were recorded on a Bruker DRX400 instrument at 400.130 MHz. Chemical shifts are reported in ppm relative to the residual solvent peak. The ^{13}C NMR spectra were recorded at 100.613 MHz and chemical shift values are reported in ppm relative to the solvent peak. Mass spectra were recorded on a JEOL SX-102A magnetic sector mass spectrometer using fast atom bombardment. Fluorimetric experiments were done on an SLM Aminco (Aminco Bowman Series 2) Luminescence Spectrometer. Vapor pressure osmometry (VPO) was performed on a Wescor 5520, Vapro instrument. Solution pH was monitored with an Orion pH-meter, model 420A, with a Ag/AgCl pH-sensitive electrode. Chromatography was performed using 60−200 mesh silica from Baker. Thin-layer chromatography was performed on Kieselgel 60 F254 and Uniplate Silica Gel GF silica-coated glass plates and visualized by UV. HPLC analysis was performed on a Shimadzu LC-10AS liquid chromatograph with a Shimadzu SPD-10 A UV−Vis detector set to 254 nm. A C-18 silica column was used as a stationary phase, and 1:1 CH_3CN:0.1% aqueous TFA was the mobile phase. Chemicals and solvents were purchased from Sigma, Fluka, Aldrich, or Acros. EYPC and cholesterol were purchased from Avanti Polar Lipids.

Synthesis. Calix[4]arene Tetramethylamide 1. Calix[4]arene tetramethylamide **1** was synthesized as described.[12]

1·HCl crystals: (a) Calix[4]arene tetramethylamide **1** (15 mg) was dissolved in 1.5 mL of THF:12 M HCl (95:5). The solution slowly evaporated to give an oily precipitate that was dissolved in 2 mL of CH_2Cl_2. Slow evaporation afforded crystals of **1**·HCl·3(H_2O). (b) Calix[4]arene tetramethylamide **1** (15 mg) was dissolved in 2 mL of CH_2Cl_2, and then 1 mL of 6 M aqueous HCl was layered over the organic solution. A white emulsion in the organic layer occurred immediately.

(38) While mammalian cells have a resting potential of −40 to −100 mV (ref 1a, p 24), *Streptococcus bovis*, the bacteria that causes endocarditis, has a transmembrane potential of up to +158 mV (positive pole inside) in the presence of glutamine, rendering this bacteria potentially susceptible to **2**. On endocarditis, see: Kupferwasser, I.; Darius, H.; Muller, A. M.; Mohr-Kahaly, S.; Westermeier, T.; Oelert, H.; Erbel, R.; Meyer, J. *Heart* **1998**, *80*, 276. On *S. bovis*, see: Cook, G. M.; Russell, J. B. *FEMS Microbiol. Lett.* **1993**, *111*, 263.

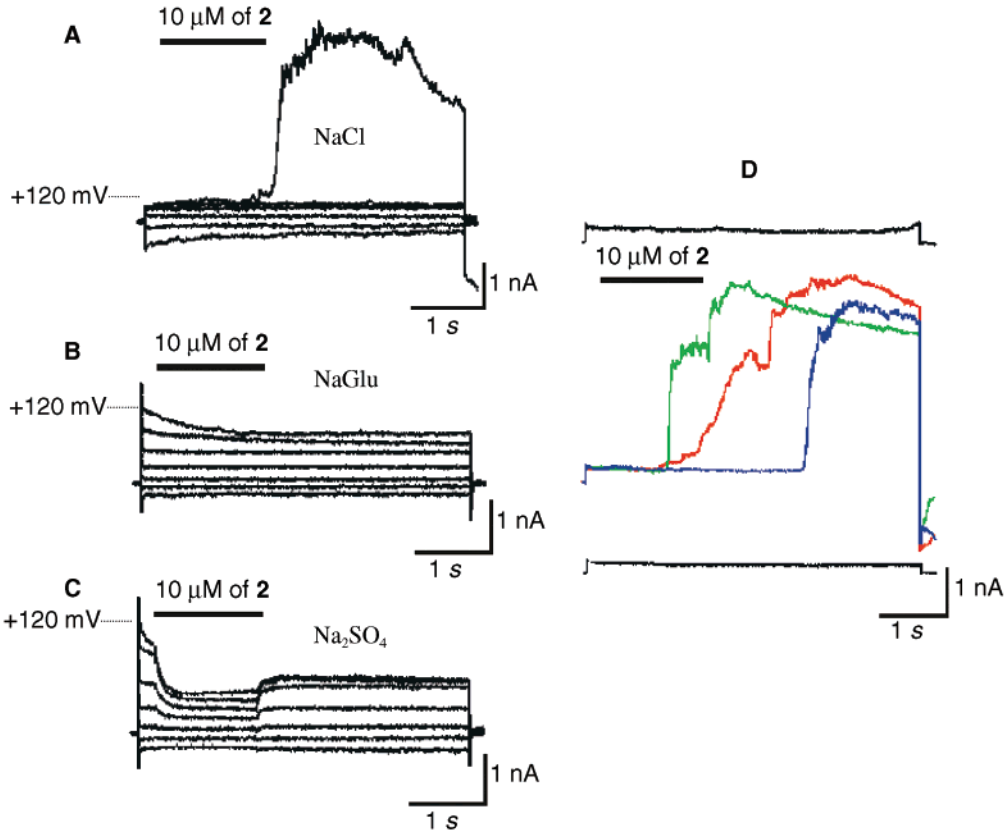

Figure 10. Voltage clamp recordings in whole cell configuration (HEK-293 cells). (A) Current across membrane after application of **2** at different voltages. From bottom to top, traces denote currents at −120, −80, −40, 0, 40, 80, 120 mV, respectively, with saline physiological buffer being used. (B) Current across membrane in a sodium glutamate isoosmotic buffer at different voltages. The potential was varied over a range of −120 through +120 mV, with a 40 mV step. (C) Current across membrane in Na_2SO_4 isoosmotic buffer at different voltages. The potential was varied over a range of −120 through +120 mV, with a 40 mV step. (D) Current across the membrane at +120 mV in application/wash cycle: traces from bottom to top denote: current in absence of **2**, current after first application of **2** (blue trace), followed by 1.5 min lavage, second application (red trace) and the third application (green trace). Trace on top designates current after lavage without further application of **2**. Baselines of the first and the last traces shifted for clarity, saline physiological buffer used.

Crystals of **1**·HCl·H_2O·CH_2Cl_2 formed at the aqueous−organic interface after several days.

Calix[4]arene tetrabutylamide 2. (a) To a suspension of tetrakis-(carboxymethoxy)-*p*-H-calix[4] arene *1,3-alt*[12] (700 mg, 1.07 mmol) in 30 mL of benzene was added 2 mL of thionyl chloride (27.4 mmol, 6.4 equiv per COOH group). The reaction mixture was stirred at reflux for 2.5 h, the solvent was evaporated under reduced pressure, and residual $SOCl_2$ was removed by coevaporation with benzene. IR spectroscopy indicated conversion of the carboxylic acid groups to acid chlorides. The acid chloride was used immediately without purification. (b) To a solution of the acid chloride in 30 mL of dry CH_2Cl_2 were added 3 mL of triethylamine (21.5 mmol, 5 equiv) and 3 mL of butylamine (30.4 mmol, 7.1 equiv). The reaction mixture was stirred overnight at room temperature and washed with water and 0.1 N HCl, and the resulting material was purified by column chromatography (silica gel, MeOH:CH_2Cl_2 4:96) to give 814 mg (0.93 mmol, 87% yield) of **2** as a white solid. ^{1}H NMR ($CDCl_3$, 25 °C) δ: 7.00 (d, J = 7.5 Hz, 8 H, ArH), 6.73 (t, J = 7.5 Hz, 4 H, ArH), 6.26 (t, J = 6.2 Hz, 4 H, CONH), 4.05 (s, 8 H, ArOCH_2CO), 3.58 (s, 8 H, ArCH_2Ar), 3.41 (m, 8 H, ArOCH$_2$CONHCH_2CH$_2$CH$_3$), 1.66 (m, 8 H, Ar−OCH$_2$−CO−NH−CH$_2$−CH_2−CH$_3$), 1.54 (m, 8 H, ArOCH$_2$CONHCH$_2$$CH_2CH_3$), 1.06 (t, J = 7.5 Hz, 12 H, ArOCH$_2$CONHCH$_2$CH$_2$$CH_3$). ^{13}C NMR ($CDCl_3$, 25 °C) δ: 167.7, 154.3, 133.9, 131.2, 122.1, 70.1, 38.8, 36.2, 32.5, 20.2, 13.9. FAB MS ([M + H]$^+$): 877.5, calcd for $C_{52}H_{69}N_4O_8$: 877.50.

Calix[4]arene Octabutylamide 3. Tetrakis(carboxymethoxy)-*p*-H-calix[4]arene[12] (423 mg, 0.65 mmol) was activated with thionyl chloride as described for **2**. To a solution of the acyl chloride in 30 mL of dry methylene chloride were added 2 mL of triethylamine (14.3 mmol, 5.5 equiv) and 3 mL of dibutylamine (17.8 mmol, 6.8 equiv). The reaction mixture was stirred overnight at room temperature and then washed with water and 0.1 N HCl, evaporated to dryness under reduced pressure, and submitted to column chromatography (silica gel, MeOH: CH_2Cl_2 6:94) to give **3**, contaminated with its Na^+ complex (determined by ^{1}H NMR). Repeated washing of this material with deionized water gave 443 mg of **3** (0.40 mmol, 62%) as a white solid. ^{1}H NMR ($CDCl_3$, 25 °C) δ: 7.16 (d, J = 8.1 Hz, 8 H, ArH), 6.67 (t, J = 7.7 Hz, 4 H, ArH), 4.41 (s, 8 H, ArOCH_2CO), 3.56 (s, 8 H, ArCH_2-Ar), 3.41 (t, J = 7.7 Hz, 8 H, ArOCH$_2$CON(CH_2)$_2$), 3.23 (t, J = 7.7 Hz, 8 H, ArOCH$_2$CON(CH_2)$_2$), 1.63−1.52 (m, 16 H, ArOCH$_2$CON-(CH$_2$$CH_2CH_2CH_3$)$_2$), 1.40−1.27 (m, 16 H, ArOCH$_2$CON(CH$_2$CH$_2$$CH_2$-CH$_3$)$_2$), 0.95 (t, J = 7.3 Hz, 12 H, ArOCH$_2$CON(CH$_2$CH$_2$CH$_2$$CH_3$)$_2$, 0.92 (t, J = 7.3 Hz, 12 H, ArOCH$_2$CON(CH$_2$CH$_2$CH$_2$$CH_3$)$_2$). ^{13}C NMR ($CDCl_3$, 25 °C) δ: 167.6, 155.39, 133.3, 129.5, 123.0, 71.7, 47.0, 45.5, 33.6, 31.2, 29.7, 20.2, 20.0, 13.9, 13.7. FAB MS ([M+H]$^+$): 1101.7, calcd for $C_{68}H_{101}N_4O_8$ 1101.75.

***N*-Butyl-2-phenoxyacetamide 4.** Phenoxyacetic acid (2 g, 13.15 mmol) was activated with $SOCl_2$ (3 mL, 41.1 mmol, 3 equiv) in 50 mL of dry benzene using the procedure described for **2**. To a solution of the acid chloride in 30 mL of dry methylene chloride were added 3 mL of Et_3N (21.5 mmol, 1.6-fold excess) and 3 mL of $BuNH_2$ (30.4 mmol, 2.3-fold excess). The reaction mixture was stirred overnight at room temperature, the solvent was evaporated to dryness under reduced pressure, and the resulting oil was dried under high vacuum. Purification by column chromatography (silica gel, MeOH:CH_2Cl_2 2:98 vv) gave 2.43 g (11.71 mmol, 89%) of **4** as a crystalline solid. ^{1}H NMR ($CDCl_3$,

25 °C) δ: 7.32 (dd, J = 8.0, 7.2 Hz, 2 H, Ar−H), 7.02 (t, J = 7.2 Hz, 1 H, ArH), 6.91 (d, J = 8.0 Hz, 2 H, ArH), 6.57 (bs, 1 H, NH), 4.48 (s, 2 H, ArOCH_2CO), 3.34 (q, J = 6.8 Hz, 2 H, NH$CH_2CH_2CH_2CH_3$), 1.50 (m, 2 H, NHCH$_2CH_2$CH$_2$CH$_3$), 1.33 (m, 2 H, NHCH$_2$CH$_2CH_2$-CH$_3$), 0.91 (t, J = 7.2 Hz, 3 H, NHCH$_2$CH$_2$CH$_2CH_3$). ^{13}C NMR ($CDCl_3$, 25 °C) δ:168.0, 157.1, 129.7, 122.0, 114.5, 67.3, 38.7, 31.5, 19.9, 13.6; MS (FAB) ([M]$^+$): 207.3, calcd for $C_{12}H_{17}NO_2$ 207.13.

Liposome Preparation. EYPC HPTS-Containing LUVs. Egg yolk L-α-phosphatidylcholine (EYPC, 60 mg, 79 μM) was dissolved in a $CHCl_3$/MeOH mixture, the solution was evaporated under reduced pressure, and the resulting thin film was dried under high vacuum for 2 h. The lipid film was hydrated in 1.2 mL of phosphate buffer (10 mM sodium phosphate, pH = 6.4, 75−100 mM M_nX, M = Na^+, K^+, Cs^+, X = Cl^-, SO_4^{2-}) containing 10 μM HPTS (pyranine, 8-hydroxypyrene-1,3,6-trisulfonic acid trisodium salt) for 2 h. The LUV suspension (1 mL) was submitted to high-pressure extrusion at room temperature (21 extrusions through a 0.1 μm polycarbonate membrane afforded LUVs with a diameter of 100 nm). The LUV suspension was separated from extravesicular dye by size exclusion chromatography (SEC) (stationary phase: Sephadex G-10, mobile phase: phosphate buffer) and diluted with the same phosphate buffer to give a stock solution with a lipid concentration of 11 mM (assuming 100% of lipid was incorporated into liposomes).

EYPC Calcein-Containing Vesicles. Calcein (224.1 mg, 0.36 mmol) was suspended in 3 mL of phosphate buffer (100 mM NaCl, 10 mM sodium phosphate, pH 6.4). The pH of the solution was adjusted to 6.4 with a 7.4 M NaOH-containing phosphate buffer, at which point all the calcein was dissolved, to give a 120 mM solution of the dye. The molality of the extravesicular buffer was adjusted to equal that of the calcein-containing solution with 1 M NaCl. Osmomolality was determined by VPO. A thin film was prepared from 60 mg of EYPC (79 μM) as described above. The lipid film was hydrated in 1.2 mL of the calcein buffer. During hydration, the suspension was submitted to five freeze−thaw cycles (dry ice in acetone, water at room temperature) and then submitted to high-pressure extrusion (21 extrusions through a 0.1 μm polycarbonate membrane afforded LUVs with an average diameter of 100 nm). Calcein-containing LUVs were separated from extravesicular dye by SEC (stationary phase: Sephadex G-25, mobile phase: extravesicular buffer with adjusted molality).

Unequally Loaded Vesicular Suspensions (intra- and extravesicular buffers are different). The molality of the extravesicular buffer was adjusted to that of intravesicular buffer by addition of a 1 M solution of the appropriate salt in phosphate buffer (molality of solutions was monitored by VPO). The pH of extravesicular buffer was adjusted to that of intravesicular buffer by addition of 1 M HCl or 1 M NaOH solution (monitored by pH meter).

Fluorimetric Transport Assays. pH-Assisted Transport Assays. Typically, 100 μL of HPTS-loaded vesicles (stock solution) was suspended in 1.85 mL of the corresponding buffer and placed into a fluorimetric cell. HPTS emission at 510 nm was monitored with excitation wavelengths at 403 and 460 nm simultaneously. During the experiment, 20 μL of a 0−10 mM THF solution of the compound of interest was added through an injection port, followed by injection of 21 μL of 0.5 M aqueous NaOH. Addition of the NaOH caused a pH increase of approximately 1 pH unit in the extravesicular buffer. Maximal changes in dye emission were obtained at the end of each experiment by lysis of the liposomes with detergent (40 μL of 5% aqueous Triton x100). The final transport trace was obtained as a ratio of the emission intensities monitored at 460 and 403 nm and normalized to 100% of transport. Pseudo-first-order rate constants were calculated from slopes of the plot of ln($[H^+_{ins}] - [H^+_{out}]$) versus time, where $[H^+_{ins}]$ and $[H^+_{out}]$ are the intravesicular and extravesicular proton concentrations. The $[H^+_{out}]$ was assumed to remain constant during the experiment, while $[H^+_{ins}]$ values were calculated for each point from the HPTS emission intensities according to the calibration equation pH = 1.1684 × log(I_o/I_1) + 6.9807 (Figure 5). The absolute values for rate constants varied depending on the age of the vesicular solution and the actual stock solution of liposomes used. Ratios between absolute values of rate constants obtained from experiments on the same batch of liposomes, however, did not vary significantly.

Calcein-Release Assay. Calcein-loaded vesicles (100 μL of the stock solution) were suspended in 1.85 mL of isoosmotic buffer and submitted to fluorescence analysis. Calcein emission was monitored at 520 nm with excitation at 490 nm. During the experiment, 20 μL of a 500 μM to 10 mM THF or THF/MeOH solution of **1** or **2** was added, followed by injection of 0−21 μL of 0.5 M aqueous NaOH and 40 μL of 5% aqueous Triton x100.

Analysis of pH Changes in the Liposomes Experiencing a Cl^- Gradient. HPTS-loaded vesicles (100 μL of the stock solution), filled with a saline phosphate buffer (10 mM sodium phosphate, pH 6.4, 100 mM NaCl), were suspended in 1.85 mL of an isoosmotic phosphate sulfate buffer (10 mM sodium phosphate, pH 6.4, ∼75 mM Na_2SO_4) and placed into a fluorimetric cell. HPTS emission at 510 nm was monitored with excitation wavelengths at 403 and 460 nm simultaneously. During the experiment, 20 μL of a 0−500 μM THF solution of the compound of interest was added through an injection port. Intravesicular pH values were obtained as a function of the ratio of HPTS emission intensities at 510 nm, when excited at 403 and 460 nm. The calibration was performed by measuring the HPTS emission intensities and the pH values of a 470 pM HPTS solution in 10 mM phosphate buffer containing 100 mM NaCl (pH was varied in the range of 5.6 through 7.6 by addition of 0.5 M NaOH or 0.5 M HCl). The calibration equation obtained (pH = 1.1684 × log(I_o/I_1) + 6.9807, r = 0.998, where I_o is the emission intensity with excitation at 460 nm and I_1 is emission intensity with excitation at 403 nm) was applied to convert the emission intensities into pH values. At the end of experiment, the aqueous compartment of liposomes was equilibrated with extravesicular solution by lysis of liposomes with detergent (40 μL of 5% aqueous Triton x100).

Electrophysiological Recordings. Patch-Clamp Experiments. HEK 293 cells, plated in 100-mm dishes containing 10 mL of the growth media, were maintained at 37 °C with 5% CO_2 in the incubator. Growth medium for HEK 293 cells was minimum essential medium supplemented with 10% fetal bovine serum, 100 U/mL penicillin and 100 μg/mL streptomycin. Electrophysiological recordings were performed in the whole-cell configuration of the patch-clamp technique using a DAGAN 8900 amplifier (Dagan Corp., Minneapolis, MN). The patch electrodes, pulled from borosilicate class capillaries, had a resistance of 3−4 MΩ when filled with internal solution containing (in mM): CsCl, 110; tetraethylammonium chloride, 20; MgATP, 5; EGTA, 14; HEPES, 20 and titrated to pH 7.4 with CsOH. Approximately 90% of electrode resistance was compensated electronically, so that effective series resistance was less than 1 MΩ. HEK cells were used for experiments 2 to 4 days after plating the cells on the cover slips. Generation of the voltage-clamp protocols and data acquisition were carried out using PCLAMP software (Axon instruments, Inc., Burlingame, CA). Sampling frequency was 0.5−2.0 kHz, and current signals were filtered at 10 kHz before digitization and storage. All experiments were performed at room temperature (23−25 °C). Cells selected for recordings had a capacitance of 25−35 pF. Cells plated on plastic cover slips (15 mm round thermanox, Nunc, Inc., Napierville, IL) were transferred to an experimental chamber mounted on the stage of an inverted microscope (Diaphot, Nikon, Nagano, Japan) and were bathed in a solution containing (in mM): NaCl, 137; $CaCl_2$, 2; KCl, 5.4; HEPES, 10; glucose, 10; $MgCl_2$, 1 (pH 7.4 adjusted with NaOH). The experimental chamber was constantly perfused at a rate of about 1 mL/min with a control bathing solution. In solutions buffered on the cell under recording KCl was omitted and in some experiments NaCl was replaced by isoosmotic amounts of Na_2SO_4 or Na glutamate. Servo-controlled miniature solenoid valves were used for rapid switching between control and test solutions (delay in solution change was

< 20 ms). Compound **2** was dissolved in DMSO, and DMSO was added in an equal amount to the control and test solutions.

Voltage-Clamp Experiments. Bilayer membranes were made from monolayers of diphytanoylphospatidylcholine (DPhPC) using the method of Montal and Mueller.[39] Recordings were made under voltage-clamp conditions using calomel electrodes with saturated KCl bridges. Solutions consisted of 1 M KCl, 1 mM $MgCl_2$, 5 mM HEPES, pH 7.0. The voltage was applied from the trans side of the lipid membrane. Once calixarene tetrabutylamide **2** was incorporated into the lipid, the current through the membrane was recorded using both a chart recorder and directly digitized and stored as a computer file. The conductance values were calculated by dividing the current by the applied voltage. The events were grouped into conductance ranges of equal magnitude for the purpose of showing the distribution of recorded conductances.

Acknowledgment. This work was supported by the National Institutes of Health and the Department of Energy (J.D.). J.D. thanks the Dreyfus Foundation for a Teacher-Scholar Award. We thank Prof. Neil Blough (University of Maryland) for use of his fluorimeter and Prof. Martin Morad (Georgetown University) for use of the electrophysiological setup. We thank Prof. Marco Colombini (University of Maryland) for access to the voltage-clamp setup, helpful discussions, and advice regarding the cell experiments. V.S. and J.D. thank Prof. Steven Rokita and Prof. Lyle Isaacs (University of Maryland) and Dr. Bruce Moyer (ORNL) for helpful comments.

Supporting Information Available: Crystallographic data including diffractometer and refinement data, final coordinates, bond lengths and angles, hydrogen bond lengths and angles, and anisotropic displacement values (PDF). Crystallographic data is also available in cif format. This material is available free of charge at http://pubs.acs.org.

JA012338E

(39) Montal, M.; Mueller, P. *Proc. Natl. Acad. Sci. U.S.A.* **1972**, *69*, 3561.